Received: 15 May 2018 | Revised: 31 August 2018 | Accepted: 12 October 2018

DOI: 10.1002/mmce.21574



WILEY INTERNATIONAL JOURNAL OF RF AND MICROWAVE COMPUTER-AIDED ENGINEERING

RESEARCH ARTICLE

# A CNTFET universal mixed-mode biquad active filter in subthreshold region

S. Mohammad Ali Zanjani[1] | Massoud Dousti[1] | Mehdi Dolatshahi[2]

[1]Department of Electrical and Computer Engineering, Science and Research Branch, Islamic Azad University, Tehran, Iran

[2]Department of Electrical Engineering, Najafabad Branch, Islamic Azad University, Najafabad, Iran

**Correspondence**
Massoud Dousti, Department of Electrical and Computer Engineering, Science and Research Branch, Islamic Azad University, Tehran, Iran.
Email: m_dousti@srbiau.ac.ir

**Abstract**

This paper presents a new low-voltage and low-power mixed-mode universal active filter, using only 12 carbon nanotube field effect transistors (CNTFETs) and 2 grounded capacitors to improve the noise performance of the proposed circuit. Due to the use of subthreshold transistors biased at ±0.2 V supply voltage, the power consumption of the proposed multi input-single output (MISO) filter is only 850 nW at 19 MHz center frequency. On the other hand, relaxing from any matching components, the center frequency and quality factor of the proposed filter can be tuned electronically with low sensitivity to the values of the active and passive elements. Furthermore, the active chip area of the proposed filter is significantly reduced to 0.047 $\mu m^2$, in 32 nm CNTFET technology. Therefore, as the HSPICE simulation results show, the input referred noise values at 19 MHz are reduced to 15.5 $nV/\sqrt{Hz}$ and 185 $fA/\sqrt{Hz}$ in voltage and current modes, respectively. It is also shown that, by changing the number of nanotubes in the CNTFET structure, a very good power-frequency trade-off can be achieved for low-power GHz applications.

**KEYWORDS**

CNTFET, low-power, mixed-mode, subthreshold, universal filter

## 1 | INTRODUCTION

In recent years, design and application of active integrated filters have been attracting more and more attentions. This is due to the fact that these filters do not require any inductor or coupling elements, resulting in more integration ability and smaller chip size. Moreover, these filters provide better electrical characteristics such as electronic tunability in comparison with the filters in passive approaches, at the cost of high sensitivity values, additional noise sources, and power consumption due to the presence of active elements in the circuit.[1–13] Therefore, designing of a mixed-mode universal filter, which generates all the filtering responses (low-pass, high-pass, band-pass, all-pass, and band-stop) with the ability of operating in both voltage and current modes is a complex task.[1–13]

Due to the increasing demands for miniaturization of portable devices as well as minimizing the power consumption in different battery powered applications, designing of subthreshold circuits in low-voltage (LV) and low-power (LP) conditions is a challenging task, which should be considered in modern electronic systems.[5,14–16] Therefore, the subthreshold technique is inevitable in low-voltage/low-power applications, especially when the supply voltage is reduced to values of less than the threshold voltage.[5,15,16]

Due to the growing problems with complementary metal oxide semiconductor (CMOS) technology, such as leakage currents, limitations in the lithographic process and quantum limitations, which appear in the minimum feature sizes under 45 nm technology, new nanometer technologies seem to be inevitable in the coming years.[15–17]

Therefore, carbon nanotube field-effect transistor (CNTFET) with MOSFET-like behavior is a promising

  

candidate for replacing the CMOS technology.[16–21] Some of the advantages of CNTFETs are: higher mobility of carriers due to the quasi-ballistic transfer, small chip size, lower intrinsic delay due to lower parasitic capacitances, better $(g_m/I_D)$ characteristics versus normalized drain current $\left[I_n = I_D/\left(\frac{W}{L}\right)\right]$. Giving the above facts, CNTFETs are widely used in the design of digital integrated circuits such as full adders and multiplexers.[19–21] Therefore, design of analog integrated circuits such as active filters in the CNTFET technology still demands much scientific effort.[16,17]

The main objective of this article is to present a new universal and mixed-mode filter that can be used as input/middle stage in the target applications such as radio-frequency identification (RFID), analog FM broadcasting, and over the horizon (OTH) radar systems.

This article is organized as follows. In Section 2, the physical structure of CNTFET as well as its circuit parameters is described. The proposed low-voltage/low-power 12-transistor CNTFET universal active filter circuit is introduced in Section 3. The performance of the proposed mixed-mode filter, which is simulated in HSPICE using 32 nm CNTFET technology, is presented in Section 4. Finally, some comparisons and conclusions are presented in Sections 5 and 6, respectively.

## 2 | CNTFET TECHNOLOGY

Carbon nanotubes are categorized into two major groups of single-walled carbon nanotube (SWCNT) and multi-walled carbon nanotube (MWCNT) structures. As it is obvious in Figure 1A, the chirality vector $(m, n)$, determines the angle of Carbon atoms along the structure, which can be considered as: armchair $(m, m)$, zigzag $(m, 0)$, and chiral for other $(m, n)$ values. Therefore, if $k$ is assumed to be an integer number, $m–n = 3k$ defines the conducting behavior for the SWCNT structure, while $m–n \neq 3k$ defines the semiconducting behavior for the CNT structure.[18–20] Therefore, assuming the lattice constant is defined as $a = 2.49$ Å, the diameter of a CNT structure $(D_{CNT})$ can be expressed as follows[16,17,19–21]:

$$D_{CNT} = \frac{a\sqrt{m^2 + n^2 + mn}}{\pi} \tag{1}$$

Figure 1B shows the physical structure of a sample CNTFET in which the semiconducting doped nanotubes are considered as the channel region, which is controlled by $V_{GS}$, similar to a typical MOSFET device.[22]

The threshold voltage $(V_T)$ of the CNTFET can be approximately expressed as Equation (2), where $q$ is the electric charge of an electron, and $V_\pi = 3.033$ eV is the carbon π–π bond energy.[16,20–22]

$$V_T \approx \frac{aV_\pi}{\sqrt{3}qD_{CNT}} \approx \frac{\pi V_\pi}{q\sqrt{3(m^2 + n^2 + mn)}} \tag{2}$$

Equation (3) expresses the CNTFET drain current in subthreshold region,[17,22–24] where $k$ is the Boltzmann constant and $R_q$ is the quantum resistance of the CNTFET. Moreover, $E_g$ is the gap energy and α is the drain optical phonon scattering (DOPS) parameter which is defined in the range of $0 < \alpha \quad 1$.

$$I_{sth} \approx \frac{kT}{qR_q}\left(\ln\left(1 + e^{\frac{2qV_{GS} - E_g}{2kT}}\right) - \ln\left(1 + e^{\frac{2qV_{GS} - 2\alpha qV_{DS} - E_g}{2kT}}\right)\right) \tag{3}$$

Consequently, the trans-conductance value of the CNTFET in subthreshold region that is considered as a relation between the output current ( $I_D$) and input voltage ($V_{GS}$) is obtained as follows[18,24,25]:

$$g_{m,sth} = \left.\frac{\partial I_{sth}}{\partial V_{GS}}\right|_{V_{ds}=0} = \frac{1}{R_q}\left(\frac{e^{\frac{2qV_{GS} - E_g}{2kT}}}{1 + e^{\frac{2qV_{GS} - E_g}{2kT}}} - \frac{e^{\frac{2qV_{GS} - 2\alpha qV_{DS} - E_g}{2kT}}}{1 + e^{\frac{2qV_{GS} - 2\alpha qV_{DS} - E_g}{2kT}}}\right) \tag{4}$$

## 3 | THE PROPOSED FILTER STRUCTURE

Regardless of implemented technology (MOSFET or CNTFET), the proposed multi input-single output (MISO) filter structure having three voltage/current inputs and one voltage/current output is shown in Figure 2. In this circuit, each pair of transistors (such as $M_1$ and $M_2$), which are

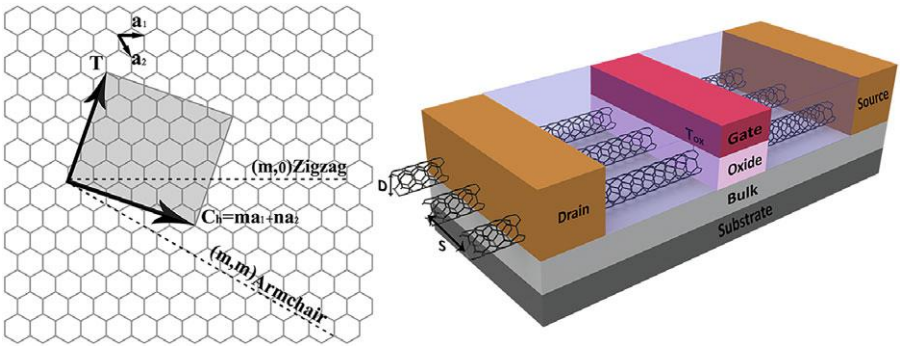


**FIGURE 1** (A) The chirality vector concept, (B) typical physical structure of a CNTFET

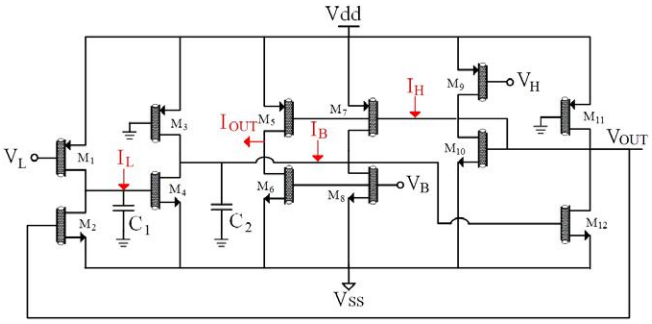


**FIGURE 2** Circuit structure of the proposed mixed-mode universal active filter

considered similar to the trans-conductance block ($G_m$), generates an output current proportional to the difference between the multiples of the input voltages. Moreover, $M_5$ and $M_6$ are considered as the *V/I* converter, which generates the output current. Therefore, the proposed circuit uses a total number of 12 transistors to implement all the filtering responses in all operating modes (voltage, current, trans-conductance, and trans-resistance) with a reduced power consumption and chip area. As it is obvious in Figure 2, the capacitors of the proposed filter are grounded; this significantly reduces the filter's parasitic effects. Additionally, $V_L$, $V_B$, and $V_H$ are the input voltages, and $I_L$, $I_B$, and $I_H$ are the corresponding input currents; $V_{out}$ and $I_{out}$ represent the output voltage and current signals, respectively.

Considering the equivalent circuit for the proposed filter structure, assuming $g_{mi}$ as the trans-conductance of $i$th transistor and $I_L = I_B = I_H = 0$, the following *voltage mode* transfer function for the proposed active filter is obtained as:

$$V_{out} = \frac{g_{m1}g_{m4}g_{m12}V_L - sC_1g_{m8}g_{m12}V_B - s^2C_1C_2g_{m9}V_H}{D(s)} \quad (5)$$

$$D(s) = s^2C_1C_2g_{m10} + sC_1g_{m7}g_{m12} + g_{m2}g_{m4}g_{m12} \quad (6)$$

In addition, the transfer function of the proposed filter in the ***trans-conductance mode*** is as follows:

$$I_{out} = g_{m5}V_{OUT} = \frac{g_{m1}g_{m4}g_{m5}g_{m12}V_L - sC_1g_{m5}g_{m8}g_{m12}V_B - s^2C_1C_2g_{m5}g_{m9}V_H}{D(s)} \quad (7)$$

Considering Equations (5)-(7), the required input configurations for implementing all the filtering responses (Low-pass, Band-pass, High-pass, Band-stop, and All-pass) by the proposed universal filter in voltage and trans-conductance modes are summarized in Table 1.

Similarly, by assuming $V_L = V_B = V_H = 0$, the following *current mode* and *trans-resistance mode* transfer functions are obtained:

$$I_{out} = \frac{g_{m4}g_{m5}g_{m12}I_L - sC_1g_{m5}g_{m12}I_B + s^2C_1C_2g_{m5}I_H}{D(s)} \quad (8)$$

**TABLE 1** Input configurations of the proposed active filter in voltage and trans-conductance modes

| Input voltage configuration | Filtering response (voltage/ trans-conductance mode) |
|---|---|
| $V_B = V_H = 0, V_L = V_{in}$ | Low pass filter |
| $V_L = V_H = 0, V_B = V_{in}$ | Band pass filter |
| $V_L = V_B = 0, V_H = V_{in}$ | High pass filter |
| $V_B = 0, V_L = V_H = V_{in}$ | Band stop filter |
| $V_B = V_H = -V_L = V_{in}$ | All pass filter |

$$V_{out} = \frac{g_{m4}g_{m12}I_L - sC_1g_{m12}I_B + s^2C_1C_2I_H}{D(s)} \quad (9)$$

Considering Equations 6, 8, and 9, the required input configurations for implementing all the filtering responses (Low-pass, Band-pass, High-pass, Band-stop, and All-pass) by the proposed universal filter in current and trans-resistance modes are summarized in Table 2.

Consequently, considering Equation 6, the center frequency ($\omega_0$) and the quality factor ($Q$) of the proposed active filter are obtained as:

$$\omega_0 = \sqrt{\frac{g_{m2}g_{m4}g_{m12}}{C_1C_2g_{m10}}} \quad (10)$$

$$Q = \frac{1}{gm_7}\sqrt{\frac{C_2g_{m2}g_{m4}g_{m10}}{C_1g_{m12}}} \quad (11)$$

Clearly, as it is obvious in Equations (10) and (11), one of the main advantages of the proposed filter is its orthogonality because the center frequency and quality factor of the proposed active filter can be tuned electronically and independent of each other. This means that the $Q$ parameter can be tuned (by adjusting $g_{m7}$) independent of $\omega_0$, as shown in Figure 7. Similarly, the $\omega_0$ parameter can be controlled by changing $g_{m2}$, $g_{m4}$, and $g_{m7}$. For example, if $g_{m2}$, $g_{m4}$, and $g_{m7}$ increase by a factor, the center frequency increases by the same factor, while the quality factor Q remains constant, as shown in Figure 8.

Moreover, for the proposed active filter, the sensitivity of $\omega_0$ and $Q$ parameters to the values of active and passive elements ($g_{mi}$ and $c_i$) are obtained as follows:

$$S_{g_{m2}}^{\omega_0} = S_{g_{m4}}^{\omega_0} = S_{g_{m12}}^{\omega_0} = 0.5 \quad (12)$$

$$S_{g_{m12}}^{\omega_0} = S_{c_1}^{\omega_0} = S_{c_2}^{\omega_0} = -0.5 \quad (13)$$

$$S_{g_{m2}}^{Q} = S_{g_{m4}}^{Q} = S_{g_{m10}}^{Q} = S_{c_2}^{Q} = 0.5 \quad (14)$$

$$S_{g_{m12}}^{Q} = S_{c_1}^{Q} = -0.5 \quad (15)$$

$$S_{g_{m7}}^{Q} = -1 \quad (16)$$

## 4 | SIMULATION RESULTS

Considering the benefits of CNTFET technology, which are discussed in Section 2, the proposed circuit is simulated in

**TABLE 2** Input configurations of the proposed universal filter in current and trans-resistance modes

| Input current configuration | Filtering response (current/ trans-resistance mode) |
|---|---|
| $I_B = I_H = 0, I_L = I_{in}$ | Low pass filter |
| $I_L = I_H = 0, I_B = I_{in}$ | Band pass filter |
| $I_L = I_B = 0, I_H = I_{in}$ | High pass filter |
| $I_B = 0, I_L = I_H = I_{in}$ | Band stop filter |
| $I_B = I_H = -I_L = I_{in}$ | All pass filter |

HSPICE using 32 nm CNTFET technology at ±0.2 V supply voltage, assuming $C_1 = C_2 = 0.1$ pF, the pitch parameter of $S$=20 nm and the chirality vector of (19, 0) with the number of nanotubes of $N$=7 for all transistors. According to Equation (2), the threshold voltage ($V_T$) is obtained as 296 mV. It is worth mentioning that all transistors are biased in subthreshold region to effectively reduce the power consumption. Figures 3 and 4 show, the simulation results for the proposed voltage and current mode universal filters at the center frequency of 19 MHz, while the whole active filter circuit consumes only 850 nW. Furthermore, Figures 5 and 6 show the simulation results of the proposed trans-conductance and trans-resistance mode filters, respectively.

As shown in Figure 7, by decreasing the number of nanotubes of $M_7$ and $M_8$, their trans-conductance values decrease and the quality factor increases, without any variation in the value of the center frequency. In addition, as it is shown in Figure 8, if $g_{m2}$, $g_{m4}$, and $g_{m7}$ increase by a factor, the center frequency $\omega_0$ also increases by the same factor, while the quality factor $Q$ remains constant.

Figure 9 shows the simulated phase-frequency response of the voltage mode all-pass filter for different values of quality factor $Q$. It is clear that by reducing the number of nanotubes of $M_7$ and $M_8$ transistors, the $g_{m7}$ parameter changes and a better phase shifting response can be obtained at a fixed center frequency value.

Equation (10) shows that the center frequency of the proposed filter is tunable by varying the trans-conductance values of the transistors or by changing $C_1$ and $C_2$ values. As an example, Figure 10 shows the sensitivity of the center frequency of the band-pass voltage mode filter to the values of capacitances $C_1$ and $C_2$.

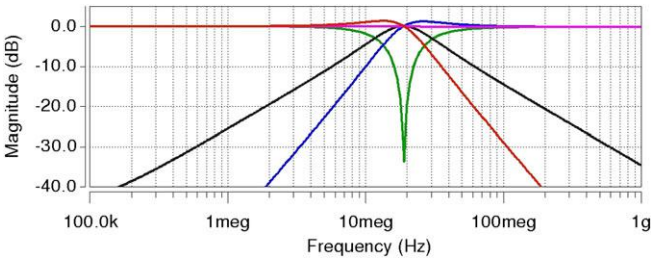


**FIGURE 3** Frequency response of the proposed voltage mode universal filter

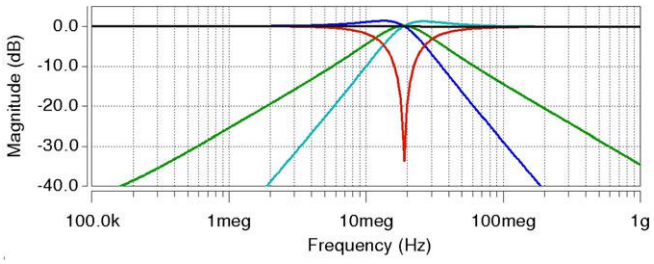


**FIGURE 4** Frequency response of the proposed current mode universal filter

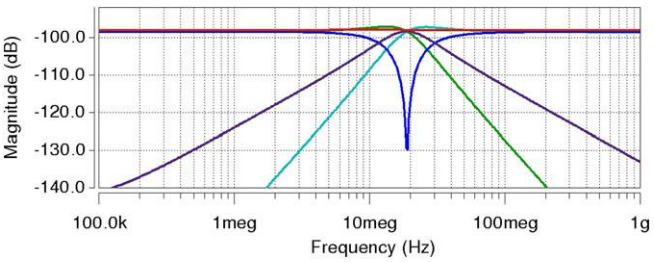


**FIGURE 5** Frequency response of the proposed trans-conductance mode universal filter

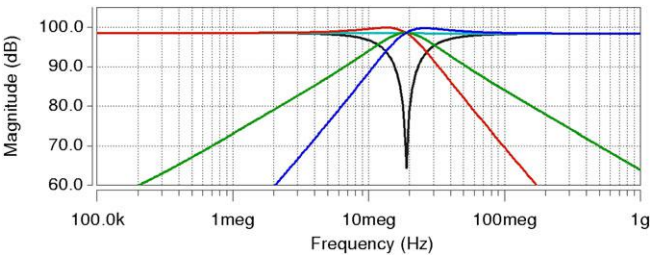


**FIGURE 6** Frequency response of the proposed trans-resistance mode universal filter

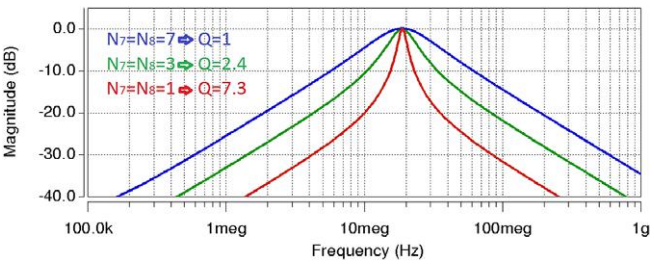


**FIGURE 7** Orthogonal tunability of quality factor at a fixed center frequency value

The thermal performance of the proposed active filter is investigated and the simulation results are presented in Figure 11, while the effect of temperature variations (in the range from −25°C to +100°C) on the center frequency and power consumption performances of the proposed filter are summarized in Table 3.

According to Equations (10) and (11), when the supply voltage increases, the trans-conductance value for all

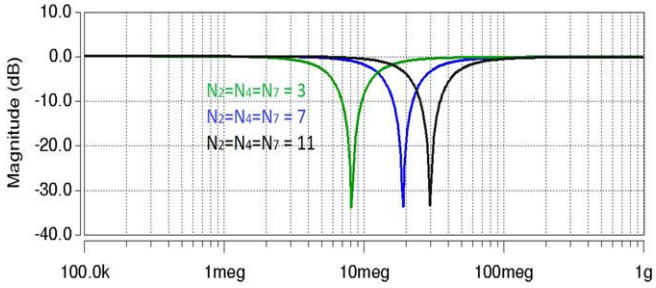


**FIGURE 8** Orthogonal tunability of center frequency at a fixed quality factor value

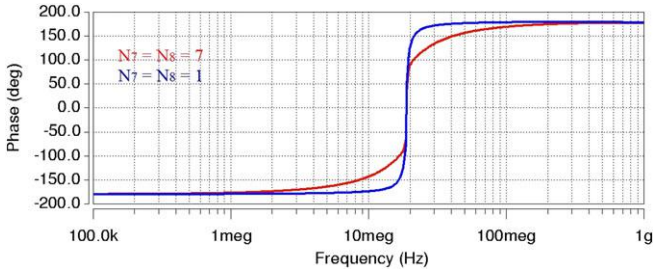


**FIGURE 9** Phase-frequency response of the voltage mode all-pass filter for different number of nanotubes

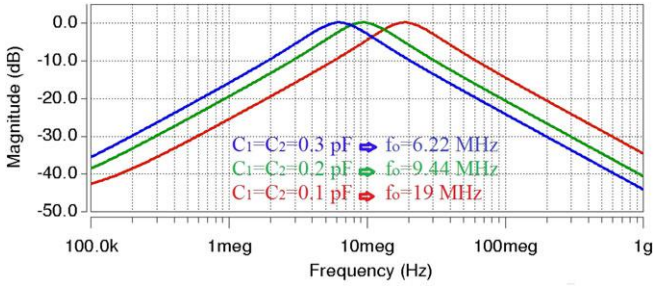


**FIGURE 10** Sensitivity of the center frequency for the band-pass voltage mode filter to the values of capacitances

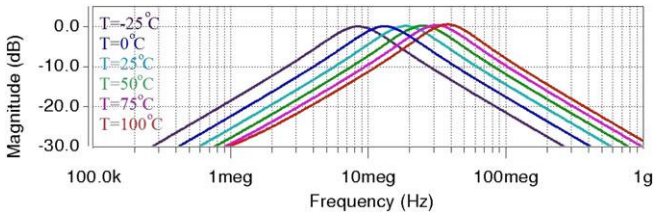


**FIGURE 11** Effect of temperature variations on the frequency response of the band-pass filter

**TABLE 3** Effect of temperature variations on the power consumption and center frequency performances of the proposed band-pass voltage mode filter at ±0.2 V supply voltage

| Temperature (°C) | −25 | 0 | 25 | 50 | 75 | 100 |
|---|---|---|---|---|---|---|
| Center frequency (MHz) | 8.6 | 13.3 | 19 | 25.5 | 31.5 | 37 |
| Power dissipation (nW) | 305 | 534 | 850 | 1250 | 1750 | 2340 |

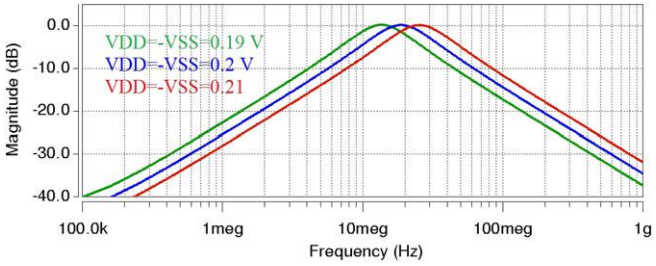


**FIGURE 12** Variation of center frequency versus supply voltage variations for the band-pass filter

**TABLE 4** Effect of supply voltage variations on the power consumption and center frequency performances of the proposed filter at 25°C

| Power supply (mV) | ±190 | ±200 | ±210 |
|---|---|---|---|
| Power consumption (nW) | 575 | 850 | 1240 |
| Center frequency (MHz) | 13.5 | 19 | 25.2 |

transistors increases as well as the center frequency of the filter; however, the quality factor remains constant. As it is shown in Figure 12 and Table 4, by varying the supply voltage from 0.19 to 0.21 V, the power consumption and center frequency of the proposed band-pass filter can be varied in the ranges of 575-1240 nW and 13.5-25.2 MHz, respectively.

The minimum input signal range can be limited by the value of the input-referred noise in all operating modes. Table 5 presents the maximum values of input referred noise for different modes of operation at a center frequency of 19 MHz. Therefore, if the amplitude of the input signal applied to the proposed filter is 1 mV or 10 pA in all modes, at the lowest possible value, it is tens of times larger than the possible amplitude of noise in the worst case.

Because the non-linear effects in active filters arise from the nonlinearities that appear in the behavior of the active elements, the overall trans-conductance of an active block is simulated in Figure 13. As it is obvious in Figure 13, the trans-conductance value for the active element in the proposed circuit structure is assumed to be approximately constant in the range of ±20 mV. It is worth mentioning that, due to the reduction of supply voltage in the subthreshold region, the input dynamic range in which the trans-conductance value remains constant is limited in comparison with other designs in strong inversion region. Giving the above facts, the total harmonic distortion (THD) parameter is reported in Table 6 for all filtering responses. As it is obvious in Table 6, for a input signal amplitude of less than

**TABLE 5** Input-referred noise values for all operating modes at 19 MHz

| Filter type | Maximum input referrred noise |
|---|---|
| Voltage mode | 15.56 nV/$\sqrt{Hz}$ |
| Current mode | 202.5 fA/$\sqrt{Hz}$ |
| Trans-conductance mode | 17 nV/$\sqrt{Hz}$ |
| Trans-resistance mode | 185 fA/$\sqrt{Hz}$ |

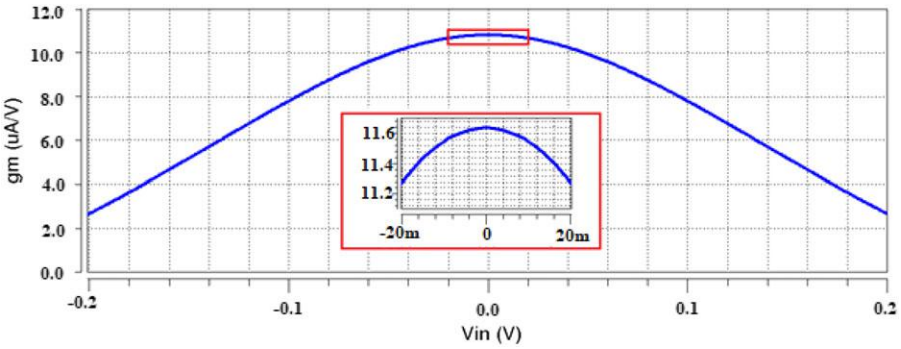


**FIGURE 13** Trans-conductance variations of the active element for different input voltages

**TABLE 6** THD values obtained for the proposed universal filter

| Filtering response | HP | LP | BP | BS | AP |
|---|---|---|---|---|---|
| THD (%) | 3.1 | 3.8 | 3.3 | 4.5 | 4.9 |

30 mVp-p, the THD parameter remains below 5%, which confirm that this circuit can be used as an input/middle stage active filter in receiver systems.

Since both drain current and trans-conductance parameters of the CNTFET depend on the number of nanotubes ($N$), the effect of changing the number of nanotubes on the variations of main performances for the proposed active filter is investigated. Table 7 and Figure 14 show that by changing the number of nanotubes in the CNTFET structure within a reasonable range, the center frequency of the filter can be changed in the order of 52.6 (from 190 MHz to 1 GHz) while the power consumption value is also increased by 5.82 (ie, in the range from 850 nW to 4.95 μW). Therefore, it is obvious that by changing the number of nanotubes, the CNTFET technology successfully implements a very good bandwidth-power trade-off in the design of low-power and high frequency active filters.

Similarly, increasing the diameter of a carbon nanotube ($D_{CNT}$) by controlling the chirality vector, shows an exponential increase in the center frequency and power consumption performances of the proposed filter, as summarized in Table 8.

In order to investigate the non-idealities effect, which arises from the process variations such as inaccurate lithographic effects and non-uniform growth of CNTs in the fabrication process on the performances of CNTFETs, the Monte-Carlo analysis is performed in HSPICE for the variations of physical parameters such as the distance between the centers of two adjacent nanotubes ($S$), and threshold voltage ($V_T$).

**TABLE 7** The effect of changing the number of nanotubes on the center frequency and power consumption performances

| Number of nanotubes (N) | 7 | 14 | 22 | 30 | 38 |
|---|---|---|---|---|---|
| $C_1 = C_2$ (fF) | 10 | 10 | 10 | 10 | 10 |
| Center frequency (MHz) | 190 | 371 | 588 | 795 | 1000 |
| Power dissipation (μW) | 0.850 | 1.69 | 2.65 | 3.63 | 4.95 |

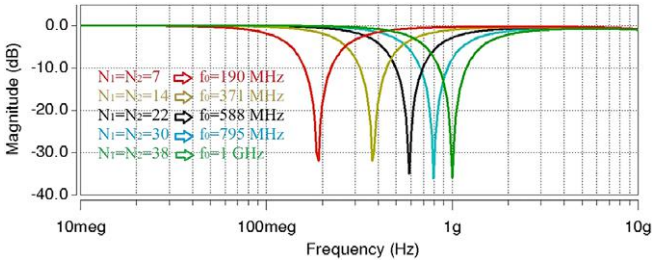


**FIGURE 14** The effect of changing the number of nanotubes on the center frequency of the proposed notch filter

Therefore, the threshold voltage variations based on ±5% Gaussian distribution with a SD of 3 are considered for 100 iterations of Monte-Carlo analysis for the CNTFET transistors. Figure 15A,B show the Monte-Carlo simulation results of the frequency response for the proposed voltage mode universal filter. Moreover, Figure 16A,B show the Monte-Carlo simulation results of the frequency response of the proposed filter for 20% variations in the pitch parameter. It is obvious that the mismatches arising from the arrangement and fabrication of CNT transistors have no significant effect on the overall performances of the proposed active filter.

## 5 | COMPARISON WITH PREVIOUS DESIGNS

Table 9 presents qualitative and quantitative comparisons between the performances of the proposed 32 nm CNTFET active filter and previous active filter designs. As it is obvious, some of the previously reported filters have some disadvantages, such as not having the capability of operating in all modes, existing dependency between the quality factor and center frequency parameters, higher number of active elements, higher power consumption for lower center frequency value and higher input-referred noise. Therefore, in order to investigate the benefits of the CNTFET technology

**TABLE 8** Effect of chirality vector variations on the performances of the proposed filter

| Chirality vector | (10, 1) | (11, 3) | (13, 0) | (11, 8) | (17, 0) | (19, 0) | (20, 2) | (30, 2) |
|---|---|---|---|---|---|---|---|---|
| $D_{CNT}$ (nm) | 0.839 | 1.012 | 1.0303 | 1.309 | 1.347 | 1.506 | 1.670 | 2.461 |
| Center frequency (MHz) | 0.0026 | 0.091 | 0.125 | 4 | 5.75 | 19 | 45.7 | 200 |
| Power consumption (nW) | 0.11 | 3.8 | 5.2 | 170 | 242 | 850 | 2243 | 17 000 |

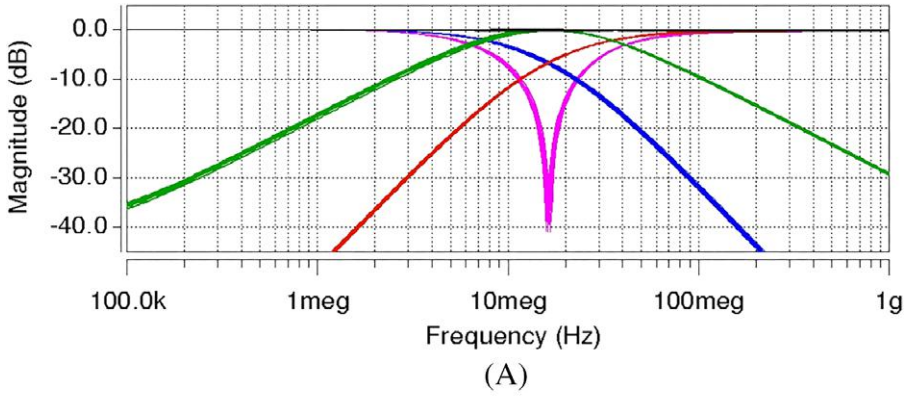


**FIGURE 15** (A) Monte-Carlo simulation results for the frequency response of the voltage mode universal filter for ±5% threshold voltage variations after 100 iterations, (B) histogram of Monte-Carlo simulation results

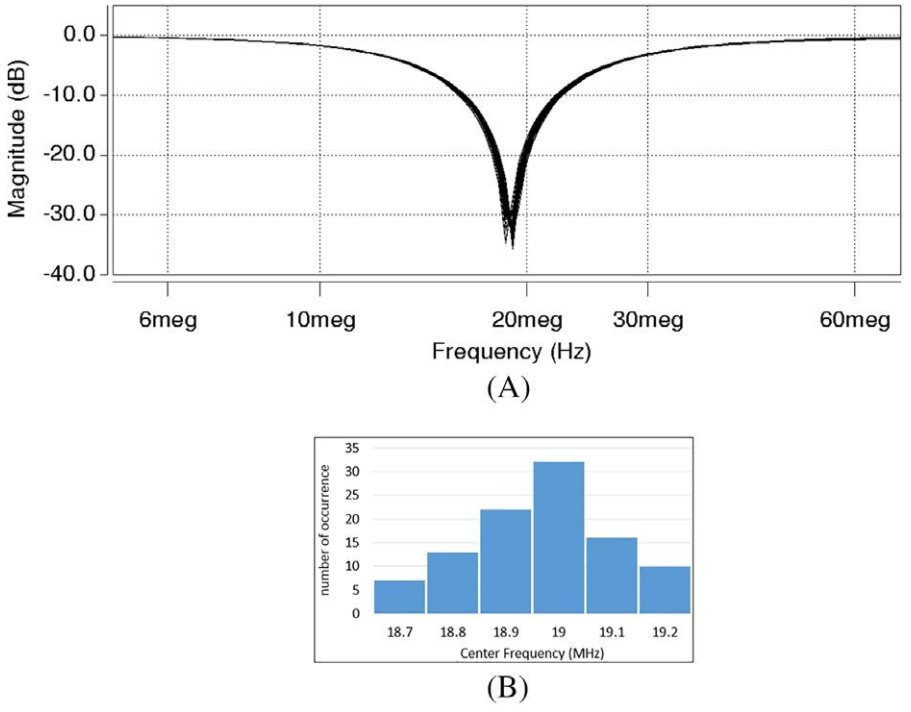


**FIGURE 16** (A) Monte-Carlo simulation results for the frequency response of the band-reject filter for 20% variations in the pitch parameter after 100 iterations, (B) histogram of Monte-Carlo simulation results

**TABLE 9** Performance comparison between the proposed active filter and previously reported designs

| Reference | 1 | 2 | 3 | 4 | 5 | 26 | Proposed circuit |
|---|---|---|---|---|---|---|---|
| Year | 2011 | 2012 | 2014 | 2017 | 2017 | 2014 | |
| Technology | 0.35 μm CMOS | 0.35 μm CMOS | 0.18 μm CMOS | 0.18 μm CMOS | 0.18 μm CMOS | 32 nm CNTFET | 32 nm CNTFET |
| Filter order | 2 | 2 | n | 2 | 2 | 2 | 2 |
| Voltage mode | ✓ | ✓ | ✓ | ✓ | ✓ | ✓ | ✓ |
| Current mode | × | ✓ | ✓ | ✓ | ✓ | ✓ | ✓ |
| Trans-conductance mode | × | ✓ | ✓ | ✓ | ✓ | × | ✓ |
| Trans-resistance mode | × | ✓ | ✓ | ✓ | ✓ | × | ✓ |
| Filter type ✓ | ✓ | ✓ | ✓ | ✓ | ✓ | ✓ | |
| ✓ | ✓ | ✓ | ✓ | ✓ | ✓ | ✓ | |
| ✓ | ✓ | ✓ | ✓ | ✓ | ✓ | ✓ | |
| ✓ | ✓ | ✓ | ✓ | ✓ | × | ✓ | |
| ✓ | ✓ | ✓ | ✓ | ✓ | × | ✓ | |
| Electronic tunability | ✓ | ✓ | × | × | ✓ | × | ✓ |
| Orthogonality | × | ✓ | × | × | × | × | ✓ |
| Subthreshold bias | × | ✓ | × | ✓ | ✓ | × | ✓ |
| Power supply | ±1.65 V | ±1.65 V | ±1.5 V | ±0.5 V | ±0.3 V | ±0.9 V | ±0.2 V |
| Power consumption | 208.25 μW | 1.57 mW | 309 μW | 75 μW | 562 nW | × | 850 nW |
| Central frequency | 10.7 MHz | 2.85 MHz | 4 MHz | 1.5 MHz | 11.48 KHz | 2.4 GHz | 19 MHz |
| Input referred noise at $f_0$ | – | – | 98 nV/$\sqrt{Hz}$ | ≥102 nV/$\sqrt{Hz}$ | ≥320 nV/$\sqrt{Hz}$ | × | ≤15.56 nV/$\sqrt{Hz}$ ≤202.5 fA/$\sqrt{Hz}$ |
| No. of transistors | 8 | 40 | 42 for $n = 2$ | 80 | 72 | 36 | 12 |

**TABLE 10** Performance comparison of the proposed active filter in MOSFET and CNTFET technologies

| Technology | VDD, VSS | Central frequency ($f_0$) | Dissipated power ($P_d$) | FOM = $\frac{f_0}{P_d.\text{Active area}}$ |
|---|---|---|---|---|
| CMOS 32 nm | ±0.5 V | 8 MHz | 1520 nW | 27 $\frac{\text{MHz}}{\mu W.\mu m^2}$ |
| CNTFET 32 nm | ±0.2 V | 19 MHz | 850 nW | 479 $\frac{\text{MHz}}{\mu W.\mu m^2}$ |

over its CMOS counterpart in terms of power-frequency trade-off, the proposed active filter is simulated in both 32 nm CMOS and CNTFET technologies and the circuit performances are obtained. Table 10, compares the simulation results of the proposed filter in both CNTFET and CMOS technologies for the same aspect ratio of transistors and assuming $C_1 = C_2 = 0.1$ pF. However, in order to perform a fair comparison, the overall circuit performance of the proposed active filter is evaluated using the following figure of merit (FOM) parameter for both technologies.

$$\text{FOM} = \frac{f_0}{P_d.\text{Active area}} \tag{17}$$

As it is obvious in Table 10, the proposed CNTFET active filter provides a better power-frequency trade-off, while it is considered as a more suitable candidate to be used in low-voltage applications.

## 6 | CONCLUSIONS

In this article, a new mixed-mode low-voltage and low-power CNTFET universal filter in subthreshold region was presented. This filter has the ability of electronic tuning of quality factor and center frequency performances orthogonally. The circuit benefits from two grounded capacitors to reduce the parasitic effects as well as the input-referred noise performance. Moreover, the circuit uses only 12 transistors in 32 nm CNTFET technology that results in an active area of only 0.047 $\mu m^2$.

Theoretical analysis and Monte-Carlo simulation results showed a low sensitivity of the quality factor and center frequency performances to the values of active and passive circuit elements (trans-conductances and capacitors) and process/ temperature variations.

## ORCID

*Massoud Dousti* http://orcid.org/0000-0002-9750-8657

## REFERENCES

1. Myderrizi I, Minaei S, Yuce E. An electronically fine-tunable multi-input–single-output universal filter. *IEEE Trans Circuit Syst II: Express Briefs*. 2011;58(6):356-360.
2. Kumngern M and Junnapiya S. Mixed-mode universal filter using OTAs. In IEEE International Conference on Cyber Technology in Automation, Control, and Intelligent Systems (CYBER), 2012.
3. Aghaei Jeshvaghani M, Dolatshahi M. A low-power multi-mode and multi-output high-order CMOS universal Gm-C filter. *Analog Integr Circuits Signal Process*. 2014;79(1):95-104.

4. Parvizi M, Taghizadeh A, Mahmoodian H, Kozehkanani ZD. A low-power mixed-mode SIMO universal Gm–C filter. *J Circuit Syst Comput*. 2017; 26(10):1750164.
5. Namdari A, Dolatshahi M. A new ultra low-power, universal OTA-C filter in subthreshold region using bulk-drive technique. *AEU-Int J Electron Commun*. 2017;82:458-466.
6. Chen H-P, Liao Y-Z, Lee W-T. Tunable mixed-mode OTA-C universal filter. *Analog Integr Circuits Signal Process*. 2009;58(2):135-141.
7. Abdalla KK, Bhaskar DR, Senani R. Configuration for realising a current-mode universal filter and dual-mode quadrature single resistor controlled oscillator. *IET Circuits Devices Syst*. 2012;6(3):159-167.
8. Maheshwari S, Singh SV, Chauhan D. Electronically tunable low-voltage mixed-mode universal biquad filter. *IET Circuits Devices Syst*. 2011;5(3): 149-158.
9. Arslanalp R, Yuce E, Tola AT. Two lossy integrator loop based current-mode electronically tunable universal filter employing only grounded capacitors. *Microelectron J*. 2017;59:1-9.
10. Safari L, Yuce E, Minaei S. A new ICCII based resistor-less current-mode first-order universal filter with electronic tuning capability. *Microelectron J*. 2017;67:101-110.
11. Abuelma'atti MT, Bentrcia A. A novel mixed-mode OTA-C universal filter. *Int J Electron*. 2005;92(7):375-383.
12. Lee C-N. Independently tunable mixed-mode universal biquad filter with versatile input/output functions. *AEU-Int J Electron Commun*. 2016;70(8): 1006-1019.
13. Sangyaem S, Siripongdee S, Jaikla W, Khateb F. Five-inputs single-output voltage mode universal filter with high input and low output impedance using VDDDAs. *Optik-Int J Light Electron Opt*. 2017;128: 14-25.
14. Khateb F, Lahiri A, Psychalinos C, Kumngern M, Kulej T. Digitally programmable low-voltage highly linear transconductor based on promising CMOS structure of differential difference current conveyor. *AEU-Int J Electron Commun*. 2015;69(7):1010-1017.
15. Khateb F, Kumngern M, Dabbous SBA, Kulej T. Low-voltage low-power bulk-driven analog median filter. *AEU-Int J Electron Commun*. 2016;70(5): 698-706.
16. Mohammad Ali Zanjani S, Dousti M, Dolatshahi M. High-precision, resistor less gas pressure sensor and instrumentation amplifier in CNT technology. *AEU-Int J Electron Commun*. 2018;93:325-336.
17. Imran A, Hasan M, Islam A, Abbasi SA. Optimized design of a 32-nm CNFET-based low-power ultrawideband CCII. *IEEE Trans Nanotechnol*. 2012;11(6):1100-1109.
18. Javey A, Tu R, Farmer DB, Guo J, Gordon RG, Dai H. High performance n-type carbon nanotube field-effect transistors with chemically doped contacts. *Nano Lett*. 2005;5(2):345-348.
19. Ebrahimi SA, Reshadinezhad MR, Bohlooli A, Shahsavari M. Efficient CNTFET-based design of quaternary logic gates and arithmetic circuits. *Microelectron J*. 2016;53:156-166.
20. Samadi H, Shahhoseini A, Aghaei-liavali F. A new method on designing and simulating CNTFET_based ternary gates and arithmetic circuits. *Microelectron J*. 2017;63:41-48.
21. Sharifi F, Moaiyeri MH, Navi K, Bagherzadeh N. Robust and energy-efficient carbon nanotube FET-based MVL gates: a novel design approach. *Microelectron J*. 2015;46(12):1333-1342.
22. Deng J, Philip Wong H-S. A compact SPICE model for carbon-nanotube field-effect transistors including nonidealities and its application—part I: model of the intrinsic channel region. *IEEE Trans Electron Devices*. 2007; 54(12):3186-3194.
23. Deng J, Philip Wong H-S. A compact SPICE model for carbon-nanotube field-effect transistors including nonidealities and its application—part II: full device model and circuit performance benchmarking. *IEEE Trans Electron Devices*. 2007;54(12):3195-3205.
24. Akinwande D, Liang J, Chong S, Nishi Y, Philip Wong H-S. Analytical ballistic theory of carbon nanotube transistors: experimental validation, device physics, parameter extraction, and performance projection. *J Appl Phys*. 2008;104(12):124514.
25. McEuen PL, Fuhrer MS, Park H. Single-walled carbon nanotube electronics. *IEEE Trans Nanotechnol*. 2002;99(1):78-85.
26. Tripathi SK and Ansari MS. Tunable active biquad filter in ±0.9V 32nm CNFET. In: IEEE Fifth International Symposium on Electronic System Design (ISED) 2014 (pp. 63–67).

## AUTHOR BIOGRAPHIES

**Sayed Mohammad Ali Zanjani** was born in Isfahan, Iran in 1972. He received the M.Sc. degree in Electronics Engineering from Islamic Azad University, Najafabad branch in 1998, respectively. Since 2000, he has been with the Department of Electrical Engineering of Najafabad Branch, Islamic Azad University. He is currently working toward the Ph.D. degree at Science and Research Branch, Islamic Azad University, Tehran, IRAN. His research interests are CNTFET and MOS, analog and digital integrated circuit design, smart home and instrumentation.

**Massoud Dousti** received B.S. in Electrical Engineering from Orleans University, Orleans, France and M.S. degrees in Electronics (Microwave and Optics) from Limoges University, Limoges, France, in 1991 and 1994 and Ph.D. in Electronics (Active Microwave Circuits) from University of Paris VI, Pierre et Marie Currie, in 1999 respectively. He served as a teaching assistant in the Department of Electrical Engineering at Ensea, Cergy Pontoise, France from 1998 to 2000. In 2001 he joined Department of Electrical Engineering of Science and Research Branch, Islamic Azad University, Tehran, IRAN, where he is now an Associate Professor. His research interests are linear and nonlinear microwave/RF circuits and systems design, millimeter wave circuit's design, and MMIC technology.

**Mehdi Dolatshahi** was born in Isfahan, Iran in 1980. He received the B.Sc. and M.Sc. degree in Electrical Engineering in 2003, 2006 respectively. He received the Ph.D. degree in Electrical Engineering in 2011from Science and Research Branch, Islamic Azad University, Tehran, Iran. He has been with the Department of Electrical Engineering of Najafabad Branch, Islamic Azad University, since 2006 where he is currently an assistant professor. His research interests include VLSI and CMOS low-voltage, low power analog and mixed-signal integrated circuit design and optimization as well as CMOS optical communications circuit design.

**How to cite this article:** Zanjani SMA, Dousti M, Dolatshahi M. A CNTFET universal mixed-mode biquad active filter in subthreshold region. *Int J RF Microw Comput Aided Eng*. 2018;e21574. https://doi.org/10.1002/mmce.21574